Chapter 2

Porous media

Groundwater is water which is stored in the soil and rock beneath the surface of the Earth. It forms a fundamental constituent reservoir of the hydrological system, and it is important because of its massive and long lived storage capacity. It is the resource which provides drinking and irrigation water for crops, and increasingly in recent decades it has become an unwilling recipient of toxic industrial and agricultural waste. For all these reasons, the movement of groundwater is an important subject of study.

Soil consists of very small grains of organic and inorganic matter, ranging in size from millimetres to microns. Differently sized (inorganic) particles have different names. Particularly, we distinguish clay particles (size < 2 microns) from silt particles (2–60 microns) and sand (60 microns to 1 mm). Coarser particles still are termed gravel.

Viewed at the large scale, soil thus forms a continuum which is granular at the small scale, and which contains a certain fraction of pore space, as shown in figure 2.1. The volume fraction of the soil (or sediment, or rock) which is occupied by the pore space (or void space, or voidage) is called the *porosity*, and is commonly denoted by the symbol ϕ; sometimes other symbols are used, for example n.

Soils are formed by the weathering of rocks, and are specifically referred to as soils when they contain organic matter formed by the rotting of plants and animals. There are two main types of rock: igneous, formed by the crystallisation of molten lava, and sedimentary, formed by the cementation of sediments under conditions of great temperature and pressure as they are buried at depth.[1] Sedimentary rocks, such as sandstone, chalk, shale, thus have their porosity built in, because of the pre-existing granular structure. With increasing pressure, the grains are compacted, thus reducing their porosity, and eventually intergranular cements bond the grains into a rock.

Igneous rock tends to be porous also, for a different reason. It is typically the case for any rock that it is fractured. Most simply, rock at the surface of the Earth

[1] There are also *metamorphic* rocks, which form from pre-existing rocks through chemical changes induced by burial at high temperatures and pressures; for example, marble is a metamorphic form of limestone.

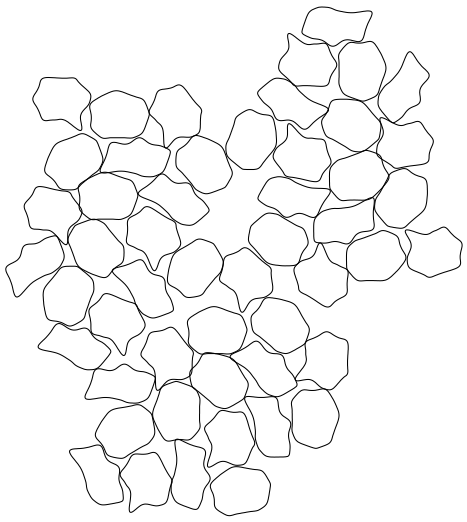

Figure 2.1: A granular porous medium.

is subjected to enormous tectonic stresses, which cause it to fold and fracture. Thus, even if the rock *matrix* itself is not porous, there are commonly faults and fractures within the rock which act as channels through which fluids may flow, and which act on the large scale as an effective porosity. If the matrix is porous at the grain scale also, then one refers to the rock as having a dual porosity, and the corresponding flow models are called double porosity models.

In the subsurface, whether it be soil, underlying regolith, a sedimentary basin, or oceanic lithosphere, the pore space contains liquid. At sufficient depth, the pore space will be saturated with fluid, normally water. At greater depths, other fluids may be present. For example, oil may be found in the pore space of the rocks of sedimentary basins. In the near surface, both air and water will be present in the pore space, and this (unsaturated) region is called the unsaturated zone, or the vadose zone. The surface separating the two is called the piezometric surface, the phreatic surface, or more simply the water table. Commonly it lies several metres below the ground surface, and more in arid regions.

2.1 Darcy's law

Groundwater is fed by surface rainfall, and as with surface water it moves under a pressure gradient driven by the slope of the piezometric surface. In order to characterise the flow of a liquid in a porous medium, we must therefore relate the flow rate to the pressure gradient. An idealised case is to consider that the pores consist of uniform cylindrical tubes of radius a; initially we will suppose that these are all aligned in one direction. If a is small enough that the flow in the tubes is laminar (this will be the case if the associated Reynolds number is $\lesssim 1000$), then Poiseuille

flow in each tube leads to a volume flux in each tube of $q = \dfrac{\pi a^4}{8\mu}|\boldsymbol{\nabla} p|$, where μ is the liquid viscosity, and $\boldsymbol{\nabla} p$ is the pressure gradient along the tube. A more realistic porous medium is *isotropic*, which is to say that if the pores have this tubular shape, the tubules will be arranged randomly, and form an interconnected network. However, between nodes of this network, Poiseuille flow will still be appropriate, and an appropriate generalisation is to suppose that the volume flux vector is given by

$$\mathbf{q} \approx -\frac{a^4}{\mu X}\boldsymbol{\nabla} p, \tag{2.1}$$

where the approximation takes account of small interactions at the nodes; the numerical tortuosity factor $X \gtrsim 1$ takes some account of the arrangement of the pipes.

To relate this to macroscopic variables, and in particular the porosity ϕ, we observe that $\phi \sim a^2/d_p^2$, where d_p is a representative particle or grain size so that $\mathbf{q}/d_p^2 \sim -\left(\dfrac{\phi^2 d_p^2}{\mu X}\right)\boldsymbol{\nabla} p$. We define the volume flux per unit area (having units of velocity) as the discharge $\mathbf{u}$. Darcy's law then relates this to an applied pressure gradient by the relation

$$\mathbf{u} = -\frac{k}{\mu}[\boldsymbol{\nabla} p + \rho g\hat{\mathbf{k}}], \tag{2.2}$$

where ρ is fluid density, g is the acceleration due to gravity, $\hat{\mathbf{k}}$ is a unit vector in the vertical (upwards) direction, and k is an empirically determined parameter called the *permeability*, having units of length squared. The discussion above suggests that we can write

$$k = \frac{d_p^2\phi^2}{X}; \tag{2.3}$$

the numerical factor X may typically be of the order of 10^3, but other assumptions can be made instead.

To check whether the pore flow is indeed laminar, we calculate the (particle) Reynolds number for the porous flow. If $\mathbf{v}$ is the (average) fluid velocity in the pore space (what we will call the *phase-averaged* velocity), then

$$\mathbf{v} = \frac{\mathbf{u}}{\phi}; \tag{2.4}$$

If a is the pore radius, then we define a particle Reynolds number based on grain size as

$$Re_p = \frac{2\rho v a}{\mu} \sim \frac{\rho|\mathbf{u}|d_p}{\mu\sqrt{\phi}}, \tag{2.5}$$

since $\phi \sim a/d_p$. Suppose (2.3) gives the permeability, and we use the gravitational pressure gradient ρg to define (via Darcy's law) a velocity scale[2]; then

$$Re_p \sim \frac{\phi^{3/2}}{X}\left(\frac{\rho\sqrt{g d_p}\, d_p}{\mu}\right)^2 \sim 10[d_p]^3, \tag{2.6}$$

[2]This scale is thus the hydraulic conductivity, defined below in (2.9).

where $d_p = [d_p]$ mm, and we have used $\phi^{3/2}/X = 10^{-3}$, $g = 10$ m s^{-2}, $\mu/\rho = 10^{-6}$ m^2 s^{-2}. Thus the flow is laminar for $d < 5$ mm, corresponding to a gravel. Only for free flow through very coarse gravel could the flow become turbulent, but for water percolation in rocks and soils, we invariably have slow, laminar flow.

In other situations, and notably for forced gas stream flow in fluidised beds or in packed catalyst reactor beds, the flow can be rapid and turbulent. In this case, the Poiseuille flow balance $-\boldsymbol{\nabla} p = \mu \mathbf{u}/k$ can be replaced by the *Ergun equation*

$$-\boldsymbol{\nabla} p = \frac{\rho |\mathbf{u}| \mathbf{u}}{k'}; \tag{2.7}$$

more generally, the right hand side will a sum of the two (laminar and turbulent) interfacial resistances. The Ergun equation reflects the fact that turbulent flow in a pipe is resisted by *Reynolds stresses*, which are generated by the fluctuation of the inertial terms in the momentum equation. Just as for the laminar case, the parameter k', having units of length, depends both on the grain size d_p and on ϕ. Evidently, we will have

$$k' = d_p E(\phi), \tag{2.8}$$

with the numerical factor $E \to 0$ as $\phi \to 0$.

Hydraulic conductivity

Another measure of flow rate in porous soil or rock relates specifically to the passage of water through a porous medium under gravity. For free flow, the pressure gradient downwards due to gravity is just ρg, where ρ is the density of water and g is the gravitational acceleration; thus the water flux per unit area in this case is just

$$K = \frac{k \rho g}{\mu}, \tag{2.9}$$

and this quantity is called the *hydraulic conductivity*. It has units of velocity. A hydraulic conductivity of $K = 10^{-5}$ m s^{-1} (about 300 m y^{-1}) corresponds to a permeability of $k = 10^{-12}$ m^2, this latter unit also being called the *darcy*.

2.1.1 Homogenisation

The 'derivation' of Darcy's law can be carried out in a more formal way using the method of homogenisation. This is essentially an application of the method of multiple (space) scales to problems with microstructure. Usually (for analytic reasons) one assumes that the microstructure is periodic, although this is probably not strictly necessary (so long as local averages can be defined).

Consider the Stokes flow equations for a viscous fluid in a medium of macroscopic length l, subject to a pressure gradient of order $\Delta p/l$. For simplicity we will ignore gravity. If the microscopic (e. g., grain size) length scale is d_p, and $\varepsilon = d_p/l$, then if we scale velocity with $d_p^2 \Delta p/l\mu$ (appropriate for local Poiseuille-type flow), length

with l, and pressure with Δp, the Navier-Stokes equations can be written in the dimensionless form

$$\begin{aligned} \boldsymbol{\nabla}.\mathbf{u} &= 0, \\ 0 &= -\boldsymbol{\nabla} p + \varepsilon^2 \nabla^2 \mathbf{u}, \end{aligned} \tag{2.10}$$

together with the no-slip boundary condition,

$$\mathbf{u} = 0 \text{ on } S : f(\mathbf{x}/\varepsilon) = 0, \tag{2.11}$$

where S is the interfacial surface. We put $\mathbf{x} = \varepsilon\boldsymbol{\xi}$ and seek solutions in the form

$$\begin{aligned} \mathbf{u} &= \mathbf{u}^{(0)}(\mathbf{x}, \boldsymbol{\xi}) + \varepsilon \mathbf{u}^{(1)}(\mathbf{x}, \boldsymbol{\xi}) \ldots \\ p &= p^{(0)}(\mathbf{x}, \boldsymbol{\xi}) + \varepsilon p^{(1)}(\mathbf{x}, \boldsymbol{\xi}) \ldots . \end{aligned} \tag{2.12}$$

Expanding the equations in powers of ε and equating terms leads to $p^{(0)} = p^{(0)}(\mathbf{x})$, and $\mathbf{u}^{(0)}$ satisfies

$$\begin{aligned} \boldsymbol{\nabla}_\xi.\mathbf{u}^{(0)} &= 0, \\ 0 &= -\boldsymbol{\nabla}_\xi p^{(1)} + \nabla_\xi^2 \mathbf{u}^{(0)} - \boldsymbol{\nabla}_x p^{(0)}, \end{aligned} \tag{2.13}$$

equivalent to Stokes' equations for $\mathbf{u}^{(0)}$ with a forcing term $-\boldsymbol{\nabla}_x p^{(0)}$. If $\mathbf{w}^j$ is the velocity field which (uniquely) solves

$$\begin{aligned} \boldsymbol{\nabla}_\xi.\mathbf{w}^j &= 0, \\ 0 &= -\boldsymbol{\nabla}_\xi P + \nabla_\xi^2 \mathbf{w}^j + \mathbf{e}_j, \end{aligned} \tag{2.14}$$

with periodic (in $\boldsymbol{\xi}$) boundary conditions and $\mathbf{u} = 0$ on $f(\boldsymbol{\xi}) = 0$, where $\mathbf{e}_j$ is the unit-vector in the ξ_j direction, then (since the equation is linear) we have (summing over j)[3]

$$\mathbf{u}^{(0)} = -\frac{\partial p^{(0)}}{\partial x_j} \mathbf{w}^j. \tag{2.15}$$

We define the average flux

$$\langle \mathbf{u} \rangle = \frac{1}{V} \int_V \mathbf{u}^{(0)} dV, \tag{2.16}$$

where V is the volume over which S is periodic.[4] Averaging (2.15) then gives

$$\langle \mathbf{u} \rangle = -\mathbf{k}^*.\boldsymbol{\nabla} p, \tag{2.17}$$

[3]In other words, we employ the summation convention which states that summation is implied over repeated suffixes, see for example Jeffreys and Jeffreys (1953).

[4]Specifically, we take V to be the soil volume, but the integral is only over the pore space volume, where $\mathbf{u}$ is defined. In that case, the average $\langle \mathbf{u} \rangle$ is in fact the Darcy flux (i. e., volume fluid flux per unit area).

where the (dimensionless) permeability tensor is defined by

$$k^*_{ij} = \langle w^j_i \rangle. \tag{2.18}$$

Recollecting the scales for velocity, length and pressure, we find that the dimensional version of (2.17) is

$$\langle \mathbf{u} \rangle = -\frac{\mathbf{k}}{\mu}.\boldsymbol{\nabla} p, \tag{2.19}$$

where

$$\mathbf{k} = \mathbf{k}^* d_p^2, \tag{2.20}$$

so that $\mathbf{k}^*$ is the equivalent in homogenisation theory of the quantity ϕ^2/X in (2.3).

2.1.2 Empirical measures

While the validity of Darcy's law can be motivated theoretically, it ultimately relies on experimental measurements for its accuracy. The permeability k has dimensions of (length)^2, which as we have seen is related to the mean 'grain size'. If we write $k = d_p^2 C$, then the number C depends on the pore configuration. For a tubular network (in three dimensions), one finds $C \approx \phi^2/72\pi$ (as long as ϕ is relatively small). A different and often used relation is that of Carman and Kozeny, which applies to pseudo-spherical grains (for example sand grains); this is

$$C \approx \frac{\phi^3}{180(1-\phi)^2}. \tag{2.21}$$

The factor $(1-\phi)^2$ takes some account of the fact that as ϕ increases towards one, the resistance to motion becomes negligible. In fact, for media consisting of uncemented (i. e., separate) grains, there is a critical value of ϕ beyond which the medium as a whole will deform like a fluid. Depending on the grain size distribution, this value is about 0.5 to 0.6. When the medium deforms in this way, the description of the intergranular fluid flow can still be taken to be given by Darcy's law, but this now constitutes a particular choice of the interactive drag term in a two-phase flow model. At lower porosities, deformation can still occur, but it is elastic not viscous (on short time scales), and given by the theory of consolidation or compaction, which we discuss later.

In the case of soils or sediments, empirical power laws of the form

$$C \sim \phi^m \tag{2.22}$$

are often used, with much higher values of the exponent (e.g. $m = 8$). Such behaviour reflects the (chemically-derived) ability of clay-rich soils to retain a high fraction of water, thus making flow difficult. Table 2.1 gives typical values of the permeability of several common rock and soil types, ranging from coarse gravel and sand to finer silt and clay.

k (m^2)	material
10^{-8}	gravel
10^{-10}	sand
10^{-12}	fractured igneous rock
10^{-13}	sandstone
10^{-14}	silt
10^{-18}	clay
10^{-20}	granite

Table 2.1: Different grain size materials and their typical permeabilities.

An explicit formula of Carman-Kozeny type for the turbulent Ergun equation expresses the 'turbulent' permeability k', defined in (2.7), as

$$k' = \frac{\phi^3 d_p}{175(1-\phi)}. \tag{2.23}$$

2.2 Basic groundwater flow

Darcy's equation is supplemented by an equation for the conservation of the fluid phase (or phases, for example in oil recovery, where these may be oil and water). For a single phase, this equation is of the simple conservation form

$$\frac{\partial}{\partial t}(\rho\phi) + \boldsymbol{\nabla}.(\rho\mathbf{u}) = 0, \tag{2.24}$$

supposing there are no sources or sinks within the medium. In this equation, ρ is the material density, that is, mass per unit volume *of the fluid*. A term ϕ is not present in the divergence term, since $\mathbf{u}$ has already been written as a volume flux (i.e., the ϕ has already been included in it: *cf.* (2.4)).

Eliminating $\mathbf{u}$, we have the parabolic equation

$$\frac{\partial}{\partial t}(\rho\phi) = \boldsymbol{\nabla}.\left[\frac{k}{\mu}\rho\{\boldsymbol{\nabla}p + \rho g\hat{\mathbf{k}}\}\right], \tag{2.25}$$

and we need a further equation of state (or two) to complete the model. The simplest assumption corresponds to incompressible groundwater flowing through a rigid porous medium. In this case, ρ and ϕ are constant, and the governing equation reduces (if also k is constant) to Laplace's equation

$$\nabla^2 p = 0. \tag{2.26}$$

This simple equation forms the basis for the following development. Before pursuing this, we briefly mention one variant, and that is when there is a compressible

pore fluid (e. g., a gas) in a non-deformable medium. Then ϕ is constant (so k is constant), but ρ is determined by pressure and temperature. If we can ignore the effects of temperature, then we can assume $p = p(\rho)$ with $p'(\rho) > 0$, and (also neglecting gravity whose effect for gases is commonly small)

$$\rho_t = \frac{k}{\mu\phi}\boldsymbol{\nabla}.[\rho p'(\rho)\boldsymbol{\nabla}\rho], \tag{2.27}$$

which is a nonlinear diffusion equation for ρ, sometimes called the *porous medium equation*. If $p \propto \rho^\gamma$, $\gamma > 0$, this is degenerate when $\rho = 0$, and the solutions display the typical feature of finite spreading rate of compactly supported initial data.

2.2.1 Boundary conditions

The Laplace equation (2.26) in a domain D requires boundary data to be prescribed on the boundary ∂D of the spatial domain. Typical conditions which apply are a no flow through condition at an impermeable boundary, $\mathbf{u}.\mathbf{n} = 0$, whence

$$\frac{\partial p}{\partial n} + \rho g \mathbf{n}.\hat{\mathbf{k}} = 0 \quad \text{on} \quad \partial D, \tag{2.28}$$

or a permeable surface condition

$$p = p_a \quad \text{on} \quad \partial D, \tag{2.29}$$

where for example p_a would be atmospheric pressure at the ground surface. Another example of such a condition would be the prescription of oceanic pressure at the interface with the oceanic crust.

A more common application of the condition (2.29) is in the consideration of flow in the saturated zone below the water table (which demarcates the upper limit of the saturated zone). At the water table, the pressure is in equilibrium with the air in the unsaturated zone, and (2.29) applies. The water table is a free surface, and an extra kinematic condition is prescribed to locate it. This condition says that the phreatic surface is also a material surface for the underlying groundwater flow, so that its velocity is equal to the average fluid velocity (*not* the flux): bearing in mind (2.4), we have

$$\frac{\partial F}{\partial t} + \frac{\mathbf{u}}{\phi}.\boldsymbol{\nabla}F = 0 \quad \text{on} \quad \partial D, \tag{2.30}$$

if the free surface ∂D is defined by $F(\mathbf{x}, t) = 0$.

2.2.2 Dupuit approximation

One of the principally obvious features of mature topography is that it is relatively flat. A slope of 0.1 is very steep, for example. As a consequence of this, it is typically also the case that gradients of the free groundwater (phreatic) surface are also small, and a consequence of this is that we can make an approximation to the equations of

groundwater flow which is analogous to that used in shallow water theory or the lubrication approximation, i. e., we can take advantage of the large aspect ratio of the flow. This approximation is called the Dupuit, or Dupuit–Forchheimer, approximation.

To be specific, suppose that we have to solve

$$\nabla^2 p = 0 \quad \text{in} \quad 0 < z < h(x, y, t), \tag{2.31}$$

where z is the vertical coordinate, $z = h$ is the phreatic surface, and $z = 0$ is an impermeable basement. We let $\mathbf{u}$ denote the horizontal (vector) component of the Darcy flux, and w the vertical component. In addition, we now denote by $\boldsymbol{\nabla} = \left(\dfrac{\partial}{\partial x}, \dfrac{\partial}{\partial y}\right)$ the horizontal component of the gradient vector. The boundary conditions are then

$$\begin{aligned} p = 0, \quad \phi h_t + \mathbf{u}.\boldsymbol{\nabla} h = w \quad \text{on} \quad z = h, \\ \frac{\partial p}{\partial z} + \rho g = 0 \quad \text{on} \quad z = 0; \end{aligned} \tag{2.32}$$

here we take (gauge) pressure measured relative to atmospheric pressure. The condition at $z = 0$ is that of no normal flux, allowing for gravity.

Let us suppose that a horizontal length scale of relevance is l, and that the corresponding variation in h is of order d, thus

$$\varepsilon = \frac{d}{l} \tag{2.33}$$

is the size of the phreatic gradient, and is small. We non-dimensionalise the variables by scaling as follows:

$$\begin{gathered} x, y \sim l, \quad z \sim d, \quad p \sim \rho g d, \\ \mathbf{u} \sim \frac{k\rho g d}{\mu l}, \quad w \sim \frac{k\rho g d^2}{\mu l^2}, \quad t \sim \frac{\phi \mu l^2}{k\rho g d}. \end{gathered} \tag{2.34}$$

The choice of scales is motivated by the same ideas as lubrication theory. The pressure is nearly hydrostatic, and the flow is nearly horizontal.

The dimensionless equations are

$$\begin{gathered} \mathbf{u} = -\boldsymbol{\nabla} p, \quad \varepsilon^2 w = -(p_z + 1), \\ \boldsymbol{\nabla}.\,\mathbf{u} + w_z = 0, \end{gathered} \tag{2.35}$$

with

$$\begin{aligned} p_z = -1 \quad \text{on} \quad z = 0, \\ p = 0, \quad h_t = w + \boldsymbol{\nabla} p.\boldsymbol{\nabla} h \quad \text{on} \quad z = h. \end{aligned} \tag{2.36}$$

At leading order as $\varepsilon \to 0$, the pressure is hydrostatic:

$$p = h - z + O(\varepsilon^2). \tag{2.37}$$

More precisely, if we put

$$p = h - z + \varepsilon^2 p_1 + \ldots, \tag{2.38}$$

then (2.35) implies

$$p_{1zz} = -\nabla^2 h, \tag{2.39}$$

with boundary conditions, from (2.36),

$$p_{1z} = 0 \quad \text{on} \quad z = 0,$$

$$p_{1z} = -h_t + |\boldsymbol{\nabla} h|^2 \quad \text{on} \quad z = h. \tag{2.40}$$

Integrating (2.39) from $z = 0$ to $z = h$ thus yields the evolution equation for h in the form

$$h_t = \boldsymbol{\nabla}.\,[h\boldsymbol{\nabla} h], \tag{2.41}$$

which is a nonlinear diffusion equation of degenerate type when $h = 0$.

This is easily solved numerically, and there are various exact solutions which are indicated in the exercises. In particular, steady solutions are found by solving Laplace's equation for $\frac{1}{2}h^2$, and there are various kinds of similarity solution. (2.41) is a second order equation requiring two boundary conditions. A typical situation in a river catchment is where there is drainage from a watershed to a river. A suitable problem in two dimensions is

$$h_t = (hh_x)_x + r, \tag{2.42}$$

where the source term r represents recharge due to rainfall. It is given by

$$r = \frac{r_D}{\varepsilon^2 K}, \tag{2.43}$$

where r_D is the rainfall rate and $K = k\rho g/\mu$ is the hydraulic conductivity. At the divide (say, $x = 0$), we have $h_x = 0$, whereas at the river (say, $x = 1$), the elevation is prescribed, $h = 1$ for example. The steady solution is

$$h = \left[1 + r - rx^2\right]^{1/2}, \tag{2.44}$$

and perturbations to this decay exponentially. If this value of the elevation of the water table exceeds that of the land surface, then a seepage face occurs, where water seeps from below and flows over the surface. This can sometimes be seen in steep mountainous terrain, or on beaches, when the tide is going out.

The Dupuit approximation is not uniformly valid at $x = 1$, where conditions of symmetry at the base of a valley would imply that $u = 0$ (below the river), and thus $p_x = 0$. There is therefore a boundary layer near $x = 1$, where we rescale the variables by writing

$$x = 1 - \varepsilon X, \quad w = \frac{W}{\varepsilon}, \quad h = 1 + \varepsilon H, \quad p = 1 - z + \varepsilon P. \tag{2.45}$$

Substituting these into the two-dimensional version of (2.35) and (2.36), we find

$$u = P_X, \quad W = -P_z, \quad \nabla^2 P = 0 \quad \text{in} \quad 0 < z < 1 + \varepsilon H, \quad 0 < X < \infty, \tag{2.46}$$

with boundary conditions

$$\begin{aligned} P = H, \quad \varepsilon H_t + P_X H_X = \frac{W}{\varepsilon} + r \quad \text{on} \quad z = 1 + \varepsilon H, \\ P_X = 0 \quad \text{on} \quad X = 0, \\ P_z = 0 \quad \text{on} \quad z = 0, \\ P \sim H \sim rX \quad \text{as} \quad X \to \infty. \end{aligned} \tag{2.47}$$

At leading order in ε, this is simply

$$\begin{aligned} \nabla^2 P = 0 \quad \text{in} \quad 0 < z < 1, \quad 0 < X < \infty, \\ P_z = 0 \quad \text{on} \quad z = 0, 1, \\ P_X = 0 \quad \text{on} \quad X = 0, \\ P \sim rX \quad \text{as} \quad X \to \infty. \end{aligned} \tag{2.48}$$

Evidently, this has no solution unless we allow the incoming groundwater flux r from infinity to drain to the river at $X = 0$, $z = 1$. We do this by having a singularity in the form of a sink at the river,

$$P \sim \frac{r}{\pi} \ln \left\{ X^2 + (1 - z)^2 \right\} \quad \text{near} \quad X = 0, \quad z = 1. \tag{2.49}$$

The solution to (2.48) can be obtained by using complex variables and the method of images, by placing sinks at $z = \pm(2n + 1)$, for integral values of n. Making use of the infinite product formula (Jeffrey 2004, p. 72)

$$\prod_1^\infty \left(1 + \frac{\zeta^2}{(2n+1)^2} \right) = \cosh \frac{\pi \zeta}{2}, \tag{2.50}$$

where $\zeta = X + iz$, we find the solution to be

$$P = \frac{r}{\pi} \ln \left[\cosh^2 \frac{\pi X}{2} \cos^2 \frac{\pi z}{2} + \sinh^2 \frac{\pi X}{2} \sin^2 \frac{\pi z}{2} \right]. \tag{2.51}$$

The complex variable form of the solution is

$$\phi = P + i\psi = \frac{2r}{\pi} \ln \cosh \frac{\pi \zeta}{2}, \tag{2.52}$$

which is convenient for plotting. The streamlines of the flow are the lines $\psi =$ constant, and these are shown in figure 2.2.

This figure illustrates an important point, which is that although the flow towards a drainage point may be more or less horizontal, near the river the groundwater seeps upwards from depth. Drainage is not simply a matter of near surface recharge and drainage. This means that contaminants which enter the deep groundwater may reside there for a very long time.

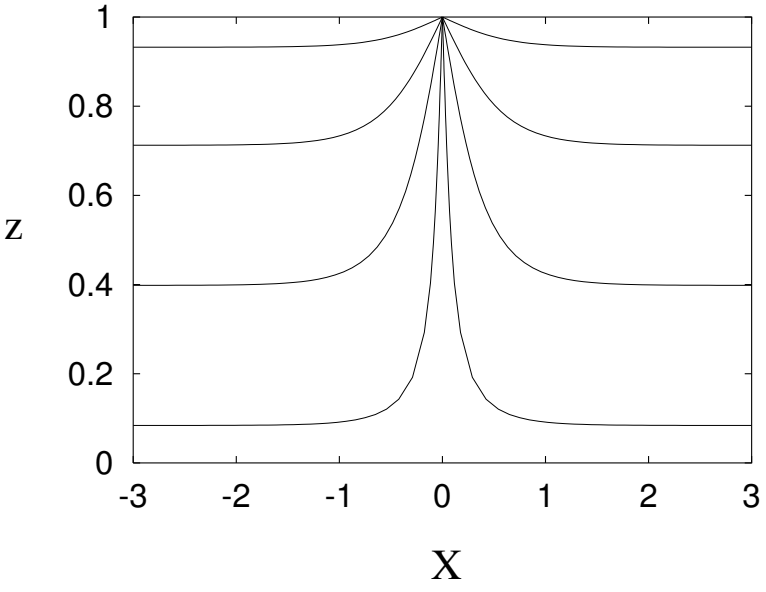

Figure 2.2: Groundwater flow lines towards a river at $X = 0$, $z = 1$.

A related point concerns the recharge parameter r defined in (2.43). According to table 2.1, a typical permeability for sand is 10^{-10} m^2, corresponding to a hydraulic conductivity of $K = 10^{-3}$ m s^{-1}, or 3×10^4 m y^{-1}. Even for phreatic slopes as low as $\varepsilon = 10^{-2}$, the recharge parameter $r \lesssim O(1)$, and shallow aquifer drainage is feasible.

However, finer-grained sediments are less permeable, and the calculation of r for a silt with permeability of 10^{-14} m^2 ($K = 10^{-7}$ m s^{-1} $= 3$ m y^{-1} suggests that $r \sim 1/\varepsilon^2 \gg 1$, so that if the Dupuit approximation applied, the groundwater surface would lie above the Earth's surface everywhere. This simply points out the obvious fact that if the groundmass is insufficiently permeable, drainage cannot occur through it but water will accumulate at the surface and drain by overland flow. The fact that usually the water table is below but quite near the surface suggests that the long term response of landscape to recharge is to form topographic gradients and sufficiently deep sedimentary basins so that this *status quo* can be maintained.

2.2.3 Saltwater intrusion in a coastal aquifer

In many dry coastal areas around the world, such as Cyprus, Israel or Australia, porous aquifers are often used as a means of storing and filtering water for safe use (e.g. drinking water). Typically, aquifers are chosen above an impermeable bed rock and are often dammed upstream to control the flow of water. Water flows towards the sea, with fresh water meeting salty water below the coastline. It is important that the salt water does not invade the aquifer since this would render the water unsuitable for supply and put the aquifer out of use for a significant time. Hence, the groundwater level is frequently monitored at various locations, and controlled by recharging if

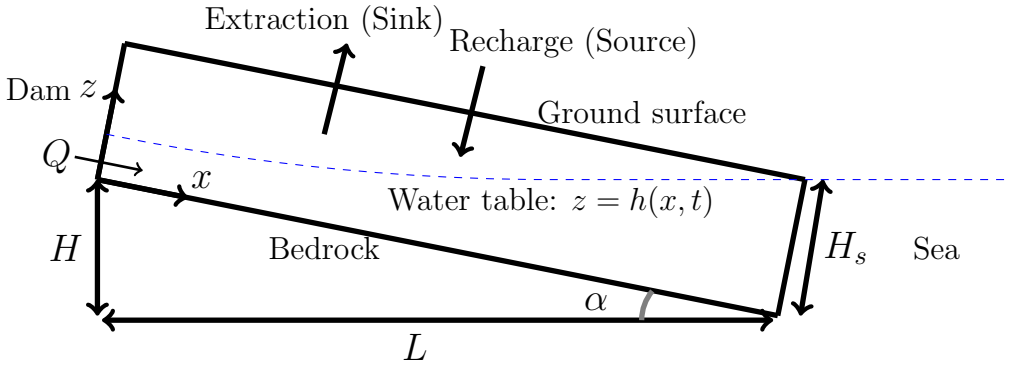

Figure 2.3: Schematic diagram of the long and thin sloping aquifer. The water table level is indicated with the blue dashed curve. The coordinate system x and z is taken respectively along and perpendicular to the bedrock, which is assumed to be flat and α is the angle to the horizontal level. (Taken from Mondal et al. (2019)).

necessary. Below the water table the aquifer is fully saturated and approximately dry above it. Here we will briefly describe and mathematically formulate such a scenario.

We choose a rotated coordinate system such that the x direction is parallel to the bedrock level, inclined at a constant angle α to the horizontal, and the z direction is perpendicular to the bedrock. L and H are the length and elevation of the aquifer, respectively, and $\tan\alpha = H/L$ (see Fig. 2.3). We denote by (u, w) the velocity components in the (x, z) directions, and by p the pressure. The flow is governed by the continuity equation and the Darcy equations as follows:

$$\begin{aligned} u_x + w_z &= 0, \\ u &= -\frac{k}{\mu}\left(p_x - \rho g \sin\alpha\right), \\ w &= -\frac{k}{\mu}\left(p_z + \rho g \cos\alpha\right). \end{aligned} \tag{2.53}$$

The rate of extraction (sinks) and recharge (sources) is modelled by a function $s(x,t)$ in the kinematic condition

$$w = h_t + uh_x - s(x,t): \quad z = h(x,t). \tag{2.54}$$

We also impose the dynamic condition $p = p_a$ on $z = h$, as well as impermeability $w = 0$ on $z = 0$, constant flux (seepage from the dam) Q at $x = 0$ and that the groundwater meets the sea level $h = H_s$ at $x = L$.

After appropriate non-dimensionalisation and using the small angle approximation $\sin\alpha \approx \alpha \approx H/L$, the governing equations and boundary conditions become

$$\begin{aligned} h_t + (h(1-h_x))_x &= s, \\ h(1-h_x) &= \hat{Q}: \quad x = 0, \\ h &= \hat{H}: \quad x = 1, \end{aligned} \tag{2.55}$$

where $\hat{Q} = QL/\epsilon KH^2$ and $\hat{H} = H_s/H$. In the steady state we can integrate this system by defining

$$S = \int_0^x s \, \mathrm{d}x, \tag{2.56}$$

which is the cumulative extraction/recharge. Hence, the dimensionless velocity of the flow is

$$1 - h_x = \frac{\hat{Q} + S(x)}{h}, \tag{2.57}$$

indicating that the outflow will be positive under the condition

$$u(x = 1) > 0 \quad \text{if} \quad \hat{Q} + S(1) > 0. \tag{2.58}$$

This imposes a constraint on the recharge rate S (given seepage rate $\hat{Q}$) such that seawater is not flowing into the aquifer (i.e. this allows water management teams to recharge sufficiently to avoid seawater intrusion). Note, in the simple case where $S = 0$ the solution is given implicitly as

$$h - \hat{H} + \hat{Q} \log \frac{h - \hat{Q}}{\hat{H} - \hat{Q}} = x - 1. \tag{2.59}$$

It is worth discussing the boundary between the fresh and salty water in more detail. In general, this boundary is modelled as being sharp (for the sake of simplicity) or diffuse, due to the transport of salt. In the case of a sharp interface model, there is a level beneath the water table, below which the water is salty (with uniform salt concentration) and above which it is completely fresh. In non-rotated coordinates (i.e. measuring z above sea level), the water table height is denoted h_w, whereas the saltwater table height is denoted h_s, such that an Archimedes balance indicates

$$h_s = \frac{\rho_w}{\rho_s - \rho_w} h_w \approx 40 h_w, \tag{2.60}$$

where ρ_s is the density of salty water. Under the small angle approximation we have

$$h_w \approx h - \left(\hat{H} + x - 1 \right), \tag{2.61}$$

where the subtracted quantity is the zero-flow case ($u = 0$). Hence, we can rearrange to find the saltwater level

$$h_s = \frac{\rho_w}{\rho_s - \rho_w} \left[h - \left(\hat{H} + x - 1 \right) \right]. \tag{2.62}$$

Again, this serves as a useful tool for estimating the intrusion of saltwater into the aquifer, and to control recharge rates accordingly to avoid contamination. In practice, the interface between these two bodies of water is not sharp, because the salt undergoes both advection and diffusion. In this case, the Boussinesq approximation can be applied to the density, such that

$$\rho = \rho_w (1 + \beta c), \tag{2.63}$$

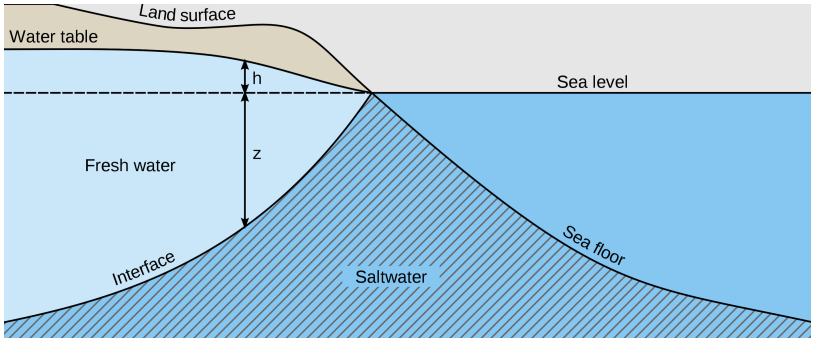

Figure 2.4: Schematic diagram of the Ghyben-Herzberg relationship for salt water intrusion in a coastal aquifer (Taken from Barlow (2003)). In (2.60) the variables h_s, h_w correspond to z, h in the image.

where β is an empirical parameter, and c is the concentration of salt which is subject to the advection-diffusion equation

$$c_t + \mathbf{u} \cdot \nabla c = D\nabla^2 c, \tag{2.64}$$

where D is the diffusion coefficient. This must be solved in conjunction with the Darcy equations, typically using a numerical scheme. In such cases, iso-levels for the concentration indicate the location of dangerous levels of saltwater intrusion.

2.2.4 Carbon capture and storage

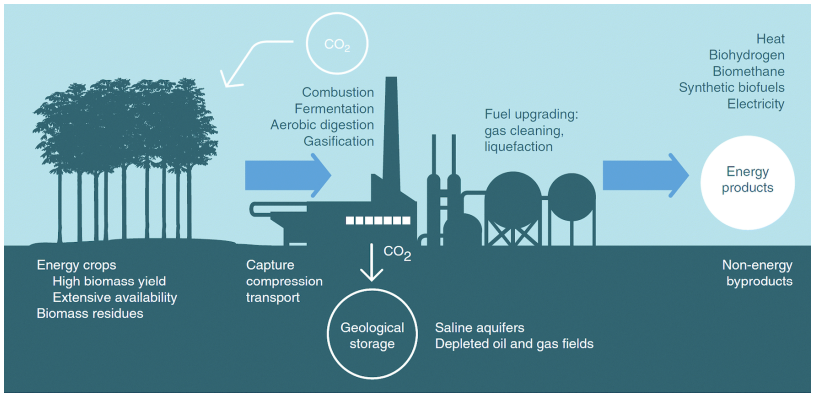

Figure 2.5: Illustration of the process of Carbon Capture and Storage (CCS). In this example, biomass (carbon sink) is combusted and CO_2 emissions captured and stored in a geological reservoir. (taken from Bui et al. (2018)).

The overproduction of carbon dioxide emissions is one of biggest challenges facing humankind over the next century. As outlined in the Paris Agreement (2015), it is

necessary to limit global warming to less than 2° C by the year 2100 to avoid the most dangerous consequences of climate change. To meet these temperature targets it is imperative to reduce our CO_2 emissions quickly, and by as much as possible.

One of the few proposed technological solutions to this problem is carbon capture and storage (CCS) - that is, capturing CO_2 at source (e.g. power plants and factories) and injecting it into porous geological reservoirs to be sequestered (stored) several kilometres beneath the ground. Trapping of the CO_2 occurs in a variety of different ways that take place over vastly different timescales, as illustrated in Fig. 2.5 (taken from Krevor et al (2015)). Initially (over the first few years of injection) the CO_2 is trapped by impermeable caprocks preventing it from rising upwards; then over longer timescales it is trapped by small scale capillary forces and by dissolution within the surrounding salty brine. Finally, over much longer time scales, the CO_2 is converted into various minerals and stored permanently in the rock.

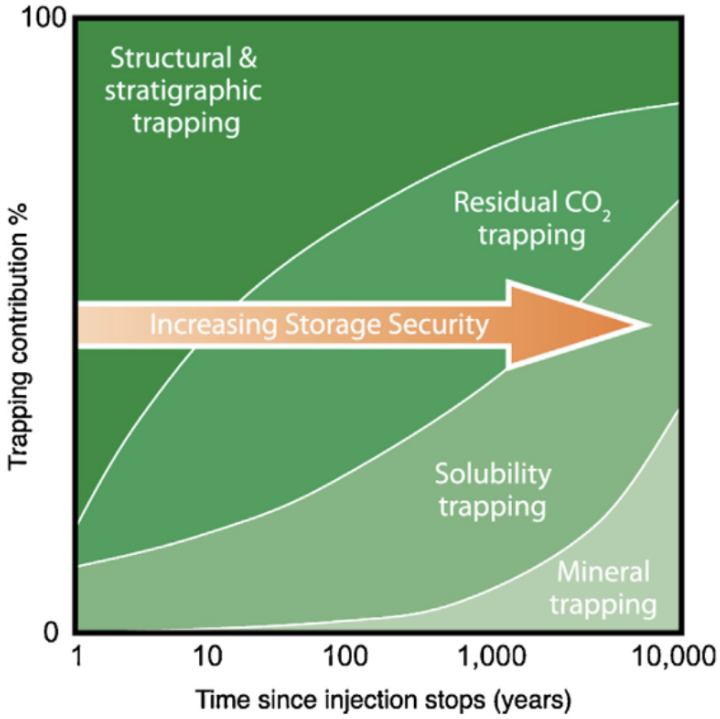

Figure 2.6: Diagram showing the different trapping mechanisms for CO_2 sequestration and the timescales over which they take place (taken from Krevor et al. (2015)).

CO_2 sequestration is currently being developed as a technology in different sites around the world. Many sites still remain in the research phase, whilst others are being designed and built to be used in conjunction with future power stations. The most famous case study of CCS is at Sleipner, a natural gas field in the Norwegian North Sea. Since 1996, after the Norwegian government introduced a significant tax on carbon emissions, the operators began capturing and sequestering CO_2 which is

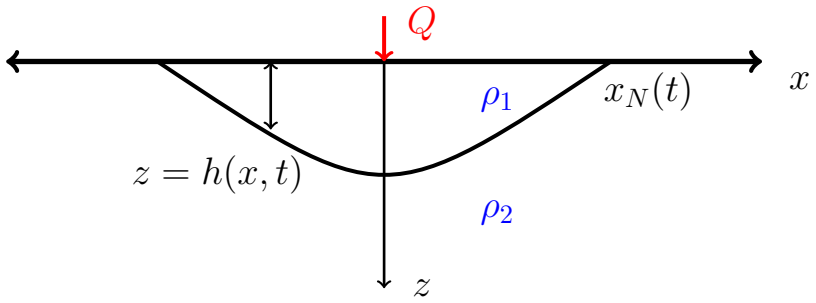

Figure 2.7: Schematic diagram of CO_2 injected at a rate Q beneath an impermeable cap rock located at $z = 0$.

extracted as a by-product of the natural gas (before this tax the CO_2 was simply released into the atmosphere). Between 1996 (when the project began) and 2018, approximately one million tonnes of CO_2 were stored at Sleipner, and it will continue to be used for many years to come.

The complex flow patterns involved during CO_2 sequestration, together with the multi-scale nature of the process (with rock variations from the millimetre to the kilometre), presents several modelling challenges. Here we discuss several useful mathematical tools, such as similarity and asymptotic analyses, to gain insights into the factors that affect CO_2 migration, and to help improve the overall safety and efficiency of CO_2 sequestration in porous geological reservoirs.

A simple illustration of CO_2 injected at a rate Q beneath an impermeable cap rock is illustrated in Fig. 2.7. For simplicity, we model this in two-dimensions (which is equivalent to CO_2 injected from a line source). The injected CO_2 has a lower density than the surrounding brine, such that $\rho_1 < \rho_2$. A coordinate system is chosen with z increasing downwards, such that the impermeable cap rock is located at $z = 0$, whereas the shape of the current is given by $z = h(x,t) \geq 0$. We consider a symmetric current and therefore restrict our attention to the half-width $x \in [0, x_N(t)]$, where $x_N(t)$ is the position of the leading edge. We denote the density difference between fluids as $\Delta\rho = \rho_2 - \rho_1$ and the conductivity as $K = k\Delta\rho g/\mu$.

By non-dimensionalising variables according to

$$x, h \sim Q/K, \quad t \sim \phi Q/K^2, \tag{2.65}$$

and applying the Dupuit approximation, the governing system of equations and boundary conditions become

$$\begin{aligned} h_t &= (hh_x)_x, \\ -hh_x &= 1, \quad x = 0, \\ -hh_x &= 0, \quad x = x_N(t), \\ h &= 0, \quad x = x_N(t). \end{aligned} \tag{2.66}$$

One of these boundary conditions can be replaced by the mass conservation condition

$$\int_0^{x_N} h \, \mathrm{d}x = t. \tag{2.67}$$

As discussed previously, such systems often admit self-similar solutions. In this case, a self-similar solution exists of the form

$$h = t^{1/3} f(\eta), \quad \eta = x/t^{2/3}, \tag{2.68}$$

for which the system reduces to a BVP of the form

$$\begin{aligned} \frac{1}{3}\left[f - 2\eta f'\right] &= \left[f f'\right]', \\ -f f' &= 1, \quad \eta = 0, \\ f &= 0, \quad \eta = \eta_N, \\ \int_0^{\eta_N} f \, \mathrm{d}\eta &= 1, \end{aligned} \tag{2.69}$$

where η_N is an unknown constant which is found as part of the solution (i.e. a free boundary problem).

2.2.5 Numerical solutions to nonlinear differential equations

Whilst we have seen such problems before, we have not yet discussed how a solution could actually be calculated. In general such problems must be solved numerically, using a finite difference scheme for example. In such a numerical approach, it is inconvenient that the size of the numerical domain (η_N) is unknown, so instead we introduce a stretched coordinate system

$$y = \eta/\eta_N, \quad F(y) = f(\eta), \tag{2.70}$$

such that the system is written as

$$\begin{aligned} \frac{\eta_N^2}{3}\left[F - 2yF'\right] &= \left[FF'\right]', \\ -\frac{1}{\eta_N} FF' &= 1, \quad y = 0, \\ F &= 0, \quad y = 1, \\ \eta_N \int_0^1 F \, \mathrm{d}y &= 1. \end{aligned} \tag{2.71}$$

Using a finite difference approach, we discretise space into N steps, $y_1, y_2, \ldots, y_N$, where $y_1 = 0$, $y_N = 1$ and $y_i - y_{i-1} = \mathrm{d}y$ is a constant step size. We denote the corresponding function values as $F_1, F_2, \ldots, F_N$, and we consider second order

accurate scheme (i.e. which solves the system up to an accuracy of $\mathcal{O}(\mathrm{d}y^2)$). There are many different possible ways we can choose to approximate derivatives using finite difference. For example, we could use a forward, central, or backward scheme, which are each given by

$$F'(y_i) \approx \frac{1}{2\mathrm{d}y}\left(-3F_i + 4F_{i+1} - F_{i+2}\right), \tag{2.72}$$

$$F'(y_i) \approx \frac{1}{2\mathrm{d}y}\left(-F_{i-1} + F_{i+1}\right), \tag{2.73}$$

$$F'(y_i) \approx \frac{1}{2\mathrm{d}y}\left(F_{i-2} - 4F_{i-1} + 3F_i\right), \tag{2.74}$$

respectively (note, these coefficients are calculated by considering a Taylor expansion about the function F evaluated at different locations). Hence, a consistent way of writing a derivative matrix $\underline{\underline{\mathbf{D}}}$ (which operates on the vector $\underline{\mathbf{F}}$) is:

$$\underline{\underline{\mathbf{D}}}\,\underline{\mathbf{F}} = \frac{1}{\mathrm{d}y}\begin{pmatrix} -3/2 & 2 & -1/2 & & \\ -1 & 0 & 1 & & \\ & & \ddots & & \\ & & -1 & 0 & 1 \\ & & 1/2 & -2 & 3/2 \end{pmatrix}\begin{pmatrix} F_1 \\ F_2 \\ \vdots \\ F_{N-1} \\ F_N \end{pmatrix}. \tag{2.75}$$

In this way, the derivative can be approximated to second order accuracy across the whole domain without using any more or fewer points than necessary. Of course, we could have used a higher (or lower) order method, in which case the above matrix would contain more (or fewer) column entries corresponding to extra terms in the Taylor series for the derivative.

The vector form of our governing equation is therefore

$$\underline{\mathbf{G}} := \frac{\eta_N^2}{3}\left[\underline{\mathbf{F}} - 2\underline{\mathbf{y}} \circ \underline{\underline{\mathbf{D}}}\,\underline{\mathbf{F}}\right] - \underline{\underline{\mathbf{D}}}\,\left[\underline{\mathbf{F}} \circ \underline{\underline{\mathbf{D}}}\,\underline{\mathbf{F}}\right] = \underline{\mathbf{0}}, \tag{2.76}$$

where the notation $\circ$ indicates the pointwise product ($\underline{\mathbf{a}} \circ \underline{\mathbf{b}} = (a_1 b_1, a_2 b_2, \ldots, a_N b_N)$). This vector equation applies to all points $i = 2, 3, \ldots N-1$, whereas the boundary conditions must be applied to the first and last points F_1 and F_N. These take the form:

$$\begin{aligned} G_1 : &= \frac{1}{\eta_N}\left[\underline{\mathbf{F}} \circ \underline{\underline{\mathbf{D}}}\,\underline{\mathbf{F}}\right]_1 + 1 = 0, \\ G_N : &= F_N = 0. \end{aligned} \tag{2.77}$$

This defines a square system of N equations ($\underline{\mathbf{G}}$) for N unknowns $\underline{\mathbf{F}}$. However, this neglects the fact that η_N is also an unknown. Hence, the mass conservation constraint provides a final equation, and we approximate this using the trapezoidal rule

$$G_{N+1} := \frac{\eta_N \mathrm{d}y}{2}\left[F_1 + F_N + \sum_{i=2}^{N-1} 2F_i\right] - 1 = 0. \tag{2.78}$$

Hence, we now have a $(N+1)\times(N+1)$ square system that is well-defined. However, we note that the governing equations and hence the system is nonlinear, and therefore cannot be solved by simple matrix inversion.

One way of solving the above system is using Newton's method. If we write the combined vector $\underline{\mathbf{X}} = (F_1, F_2, \ldots, F_N, \eta_N)$, then Newton's method provides iterations for converging to the root of the function $\underline{\mathbf{G}}(\underline{\mathbf{X}})$. Starting with an initial guess $\underline{\mathbf{X}}^0$, iterations are thereafter given by

$$\underline{\mathbf{X}}^{n+1} = \underline{\mathbf{X}}^n - \underline{\underline{\mathbf{J}}}^{-1}(\underline{\mathbf{X}}^n)\underline{\mathbf{G}}(\underline{\mathbf{X}}^n), \tag{2.79}$$

where $\underline{\underline{\mathbf{J}}}$ is the Jacobian matrix. The Jacobian is defined (using subscript notation) as

$$J_{ij} = \frac{\partial G_i}{\partial X_j}. \tag{2.80}$$

There are several ways we could calculate $\underline{\underline{\mathbf{J}}}$. In principle, none of the individual $\underline{\mathbf{G}}$ equations are very complicated, so it's feasible to calculate these analytically. However, this is extremely tedious and prone to error, considering the number of equations involved (i.e. for large N). Hence, one approach is to calculate $\underline{\underline{\mathbf{J}}}$ using finite differences, by evaluating $\underline{\mathbf{G}}$ at different values of $\underline{\mathbf{X}}$. However, since $\underline{\mathbf{G}}$ and $\underline{\mathbf{X}}$ are both of length $N+1$, this requires $(N+1)^2$ function evaluations per Newton iteration. In other words, this becomes intractable for large N. However, for smaller values of N (as we will see in Problem Sheet 2), this works fine.

Another approach is to use a computer to calculate the derivatives in $\underline{\underline{\mathbf{J}}}$ for us, which is known as *automatic differentiation*. This is an extremely powerful (but surprisingly seldom used) tool. The idea is that all variables written in computer code are defined in terms of operations like multiplication, addition, and so on, which can all be differentiated by the chain and product rules. Even more complicated functions such as $\sin(x)$, $\exp(x)$, etc... are usually defined in terms of a Taylor series on a computer, and therefore are simply defined in terms of addition and multiplication. In this way, a computer can compile the Jacobian matrix in terms of a very long list of chain rule operations given in terms of the variables $\underline{\mathbf{X}}$. This only needs to be compiled once (before running the code) and can thereafter be evaluated at every iteration. For example, the 1$^{\text{st}}$ row of $\underline{\mathbf{G}}$ is

$$G_1 = \frac{1}{2\eta_N \mathrm{d}y} F_1 \left(-3F_1 + 4F_2 - F_3\right) + 1. \tag{2.81}$$

It is straightforward for a computer to calculate derivatives of G_1 using the product and chain rule. For example, the first entry of the Jacobian (as seen by an automatic differentiation algorithm) is

$$\frac{\partial G_1}{\partial F_1} = \frac{1}{2\eta_N \mathrm{d}y}\frac{\partial F_1}{\partial F_1}\left(-3F_1 + 4F_2 - F_3\right) + \frac{1}{2\eta_N \mathrm{d}y} F_1 \left(-3\frac{\partial F_1}{\partial F_1} + 0 - 0\right) + 0. \tag{2.82}$$

Automatic differentiation is a feature of the *Julia* programming language, for example (see Problem Sheet 2).

Another approach to solve such problems is known as the *shooting method*. This is where we convert the above BVP into an IVP and guess the value of $\eta_N = \eta_{N_0}$. First we note that we can write the problem as a system of first order ODE's,

$$\begin{aligned} F'(y) &= -\frac{L}{F}, \\ L'(y) &= -\frac{\eta_N^2}{3}\left(F + 2y\frac{L}{F}\right), \end{aligned} \tag{2.83}$$

where we have introduced the flux function $L = -FF'$. At the right hand boundary the variables satisfy

$$L(1) = 0, \quad F(1) = 0, \quad \lim_{y\to 1}\frac{L}{F} = \frac{2\eta_N^2}{3}, \tag{2.84}$$

where the last of these is found by analysing the governing ODE's near $y \approx 1$. One can then discretise the variables $\underline{\mathbf{F}}$, $\underline{\mathbf{L}}$, into N points, as before. Then, the solution is found by marching backwards from $y = 1$ down towards $y = 0$ using a suitable finite difference scheme. For example, a simple first order scheme gives us

$$\begin{aligned} F_{i-1} &= F_i - \mathrm{d}y\left[-\frac{L}{F}\right]_i, \\ L_{i-1} &= L_i - \mathrm{d}y\left[-\frac{\eta_N^2}{3}\left(F + 2y\frac{L}{F}\right)\right]_i, \end{aligned} \tag{2.85}$$

which can be evaluated for $i = N, N-1, \ldots, 2$. Hence, the flux value at the origin, L_1 will not satisfy the correct condition $L_1 = \eta_N$ unless the correct value of η_{N_0} was used as an initial guess. Equivalently, the same applies to the mass conservation condition (2.67) (which is (2.78) in discretised form).

This is why the above approach is known as the shooting method. A guess is chosen for the parameter η_{N_0}, after which one shoots towards the origin (missing one's target), and η_N is updated accordingly to get closer and closer to the target iteratively. Essentially, we treat the above approach as a root-finding method for the function

$$\mathcal{F}(\eta_N) = \eta_N \int_0^1 F\,\mathrm{d}y - 1, \tag{2.86}$$

where the integral is discretised (e.g. using the trapezoidal rule) and the vector $\underline{\mathbf{F}}$, which is calculated numerically using the shooting method, is considered a function of the parameter η_N. Hence, η_N can be updated using any root-finding algorithm, such as Newton's method for example.

Whilst these examples give two possible approaches to solve nonlinear differential equations, there are plenty of other methods, such as *pseudo-time-stepping*, for example. Let's briefly discuss time-stepping methods in general, since these are essential in most fluid dynamics problems. Suppose that the boundary conditions of the above problem were modified in such a way that no self-similar solution exists. For example,

this can be achieved by setting the inflow condition to some function of time $Q = Q(t)$ which is not necessarily power law (e.g. set by the operator of the CO_2 sequestration site). In this case it is not possible to convert to a set of similarity equations, but instead we must solve the full PDE system (2.66) numerically. However, there is no need to fear since we already have nearly all the tools to do this.

First we discretise the shape of the current into a vector of N spatial points, $\underline{\mathbf{h}}$. Then, we discretise in time by considering a time step of size $\mathrm{d}t$ and marching forwards from $t = 0$ to the n^{th} time step value, $t = n\mathrm{d}t$. Approximating the time derivative using a first order implicit Euler scheme, we get

$$\frac{1}{\mathrm{d}t}\left(\underline{\mathbf{h}}^{n+1} - \underline{\mathbf{h}}^{n}\right) = (\underline{\underline{\mathbf{D}}}\,\underline{\mathbf{h}}^{n+1}) \circ (\underline{\underline{\mathbf{D}}}\,\underline{\mathbf{h}}^{n+1}) + \underline{\mathbf{h}}^{n+1} \circ (\underline{\underline{\mathbf{D}}}^2\,\underline{\mathbf{h}}^{n+1}). \tag{2.87}$$

This is known as an implicit scheme because the right hand side is evaluated at the $n+1$ time step, rather than the n time step, which is far more stable (see any standard textbook on numerical analysis). Hence, the above can be rearranged into a system of equations for the unknown vector $\underline{\mathbf{h}}^{n+1}$, which are

$$\underline{\mathbf{G}}(\underline{\mathbf{h}}^{n+1}) := \underline{\mathbf{h}}^{n+1} - \underline{\mathbf{h}}^{n} - \mathrm{d}t\left[(\underline{\underline{\mathbf{D}}}\,\underline{\mathbf{h}}^{n+1}) \circ (\underline{\underline{\mathbf{D}}}\,\underline{\mathbf{h}}^{n+1}) + \underline{\mathbf{h}}^{n+1} \circ (\underline{\underline{\mathbf{D}}}^2\,\underline{\mathbf{h}}^{n+1})\right], \tag{2.88}$$

where $\underline{\mathbf{h}}^{n}$ is known. This approach is often called the *method of lines*.

As before, we need to ensure that the boundary conditions are satisfied at $x = 0$ and $x = x_N(t)$. The flux boundary condition at $x = 0$ is imposed by replacing the first equation in (2.88) with

$$G_1 := \left[\underline{\mathbf{h}}^{n+1} \circ (\underline{\underline{\mathbf{D}}}\,\underline{\mathbf{h}}^{n+1})\right]_1 + Q^{n+1} = 0, \tag{2.89}$$

where Q^{n+1} is the function $Q(t)$ discretised and evaluated at the $n+1$ time step.

The boundary conditions at $x = x_N(t)$ can be dealt with using a special trick, making use of the fact that the shape function $h(x,t)$ has *compact support*. In other words, for $x \geq x_N(t)$ the shape satisfies $h = 0$, and $-hh_x = 0$ exactly. Therefore, if we define our numerical domain $x \in [0, L]$ and discretise into N points h_i, then we can set the initial conditions for the gravity current as

$$h_i^0 = \begin{cases} f(x_i): & 0 < x_i < x_N(0), \\ 0: & x_N(0) \leq x_i \leq L, \end{cases} \tag{2.90}$$

for some function f which is continuous at the initial nose position $x = x_N(0)$. Henceforth, for all time steps $n > 0$ we solve the nonlinear square system (2.88) (with first entry (2.89)) using Newton's method, and there is no need to impose any boundary conditions at $x = x_N$. This is because the flux $-hh_x$ naturally vanishes wherever the thickness h drops to zero, i.e. at the moving boundary $x_N(t)$. There is no need to impose the dynamic evolution of $x_N(t)$, since this will naturally follow from conservation of mass (i.e. since the PDE and BC's are satisfied). This method can be applied to many diffusion problems with compact support, and we will explore further in Problem Sheet 2.

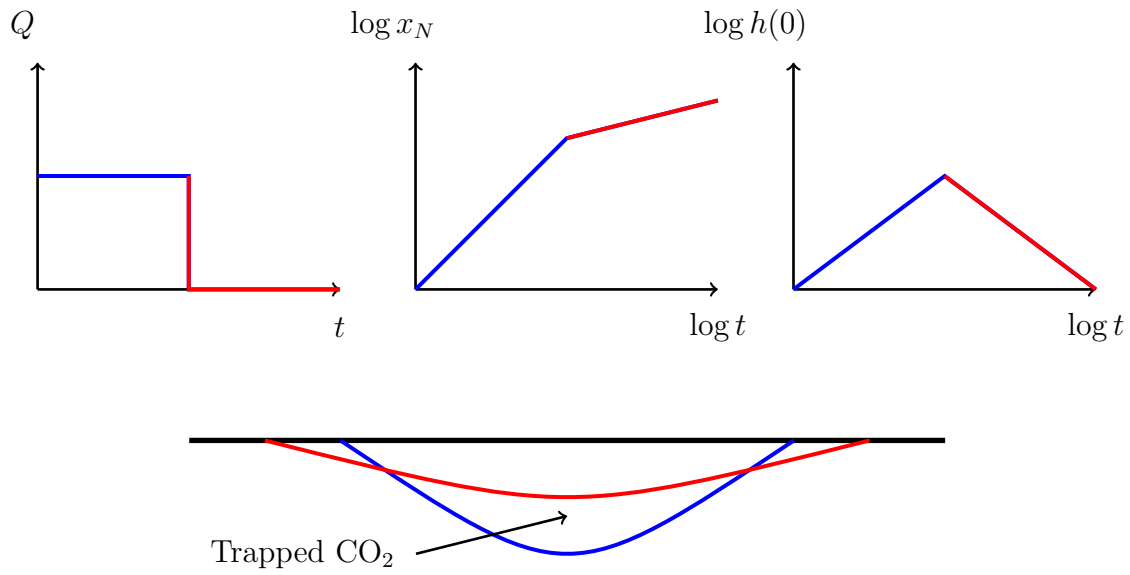

Figure 2.8: Illustration of gravity current dynamics when CO_2 is injected over an interval.

2.2.6 Injection intervals

Suppose that at some time after injection the flow rate is switched off $Q = 0$. In this case, conservation of mass indicates that the gravity current must satisfy

$$\int_0^{x_N(t)} h \, \mathrm{d}x = V, \tag{2.91}$$

for all time thereafter, where V is some constant. It is straightforward to show that this setup admits a similarity solution of the form

$$h = t^a f(\eta), \quad \eta = x/t^b, \tag{2.92}$$

where $a = -1/3$ and $b = 1/3$. Attention must be paid when considering the non-dimensionalisation of this model, since Q no longer exists as a dimensional parameter. Instead, appropriate scalings are given in terms of the volume (per unit width) of the current

$$x, h \sim V^{1/2}, \quad t \sim \phi V^{1/2}/K. \tag{2.93}$$

We note that the vertical extent of the current h shrinks like $\sim t^{-1/3}$ when $Q = 0$, compared to growing like $\sim t^{1/3}$ when Q is a constant. Hence, if we consider an injection interval in which Q is switched off after some finite time t_c, then the motion of the current changes from a situation in which it is invading new vertical space to a situation in which it is withdrawing from that vertical space. As we will discuss later, due to contact line effects between the CO_2, rock and water, the invading and retreating properties of CO_2 are different. In fact, as the CO_2 withdraws from pore

space, it typically leaves a fraction of its mass behind, trapped in the pore spaces due to small scale capillary forces. This scenario is illustrated in Fig. 2.8, indicating the region of trapped CO_2 as the injection switches off. Since the objective of CCS is to sequester as much CO_2 as possible within a reservoir, there is an important and active area of research in understanding ways to optimally store CO_2 by controlling injection rates in such ways.

2.2.7 Heterogeneities

Figure 2.9: Tullig point, Co. Clare, Ireland. (taken from Woods (2005)).

So far we have only considered spatially uniform rocks with constant permeability k and porosity ϕ. In practice, all real porous media in the environment have significantly non-uniform values of k and ϕ. For example, rocks are often composed of sedimentary layers, as can be seen on some coastal cliffs. Such rocks were formed by the deposition of different types of sediment over time, resulting in layers with potentially very different properties (such as permeability), as shown in Fig. 2.9. When considering flow of CO_2, groundwater, or any such fluid through a heterogeneous rock, the resulting patterns can become extremely complex and difficult to resolve. Hence, it is often desirable to describe the averaged, or *upscaled*, properties of heterogeneous porous media, rather than modelling the precise details of these complex layer arrangements. Here we will briefly discuss some approaches for upscaling heterogeneous media, and how these heterogeneities can affect the macroscopic arrangement of the flow.

Consider the two flow scenarios depicted in Fig. 2.10. A constant pressure drop $p_b - p_a$ is imposed across a layered rock of width L. We consider separately the flow perpendicular to, and parallel to a two layer system with permeability values k_1 and

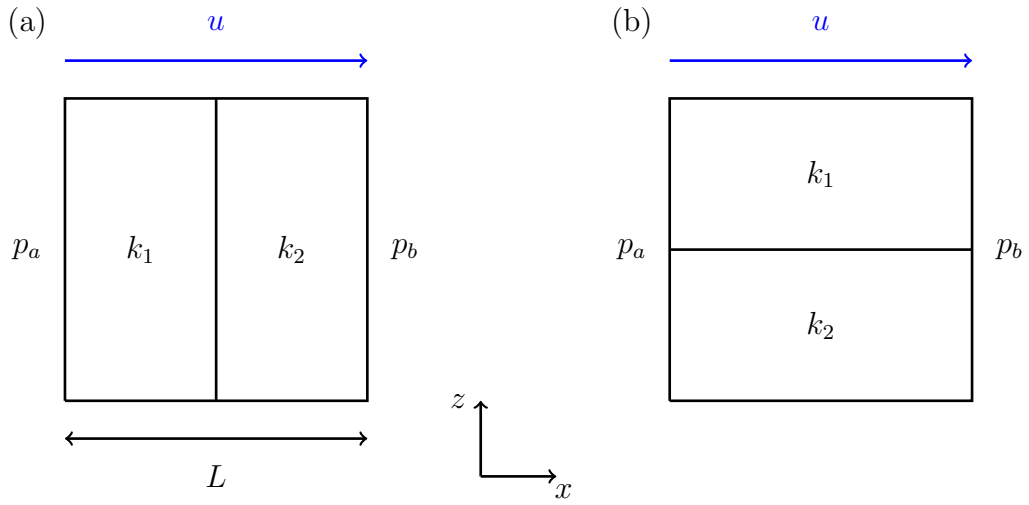

Figure 2.10: Schematic diagram of flow perpendicular (a) and parallel (b) to sedimentary layers in a porous rock.

k_2. Starting with the first (perpendicular) case, Darcy's law states that the horizontal flow is given by

$$u = -\frac{k(x)}{\mu} p_x. \tag{2.94}$$

By integrating across the width of the flow region, we get

$$\Delta p = p_b - p_a = \int_0^L -\frac{\mu u}{k(x)}\, \mathrm{d}x. \tag{2.95}$$

Meanwhile, the continuity equation $u_x + w_z = 0$ indicates that if there is no vertical flow then u must be a constant. By symmetry (or by considering an infinitely tall system) we see that $w = 0$, and hence the above integral simplifies and rearranges to

$$u = -\frac{k_\perp \Delta p}{\mu L}, \tag{2.96}$$

where the effective permeability in the perpendicular direction is given by

$$k_\perp = \frac{2}{1/k_1 + 1/k_2}, \tag{2.97}$$

which is incidentally the harmonic mean of the two permeability values. Since u is a constant in this system, it is also equivalent to the average velocity value, and hence we write $u = \bar{u}$.

In the case of flow parallel to the layers (as shown in Fig. 2.10b), the horizontal flow is different in each of the two layers

$$\begin{aligned} u_1 &= -\frac{k_1 \Delta p}{\mu L}, \\ u_2 &= -\frac{k_2 \Delta p}{\mu L}. \end{aligned} \tag{2.98}$$

Hence, the average flow across the system is given by

$$\bar{u} = -\frac{k_\parallel \Delta p}{\mu L}, \tag{2.99}$$

where

$$k_\parallel = \frac{1}{2}(k_1 + k_2). \tag{2.100}$$

We now have two effective permeability values for flow perpendicular and parallel to the layers. In this way, we can define the ratio between the two as

$$\alpha = \frac{k_\perp}{k_\parallel} = \frac{4\kappa}{(1+\kappa)^2}, \tag{2.101}$$

where $\kappa = k_1/k_2$. Clearly, $\alpha(\kappa)$ has a unique maximum at $\kappa = 1$. This indicates that perpendicular flow is always less than parallel flow for a fixed pressure gradient and viscosity.

In general, these upscaled permeability values are a good approximation for flow across or along many-layered systems, so long as the flow length scale h is much larger than the layer width scale d, such that $h/d \gg 1$. In other words, a unidirectional flow across a system of many layers can be well approximated as a flow through a homogeneous medium with uniform permeability given by $k_\perp$.

In the case where the flow has more complex layer structures (i.e. with more than two permeability values, or with differing layer widths), the above upscaling analysis can be extended easily. In this case, we have

$$\begin{aligned} k_\perp &= \left[\frac{1}{L}\int_0^L \frac{1}{k}\,\mathrm{d}x\right]^{-1}, \\ k_\parallel &= \frac{1}{H}\int_0^H k\,\mathrm{d}z, \end{aligned} \tag{2.102}$$

where H is the vertical extent of the flow region.

For real sedimentary systems the ratio $\alpha(\kappa)$ has been measured in the range $10^{-4} - 10^{-1}$. Next we will investigate the possible consequences of such a large permeability ratio. To do so, we consider a porous medium with upscaled properties $k_\parallel$ and $k_\perp$ in the x and z directions. This is known as an *anisotropic* permeability field, for which Darcy's law is written

$$\mathbf{u} = -\frac{1}{\mu}\underline{\underline{\mathbf{k}}} \cdot \nabla\left[p + \rho g z\right], \tag{2.103}$$

where $\underline{\underline{\mathbf{k}}} = \mathrm{diag}(k_\parallel, k_\perp)$. In doing so, we have approximated a heterogeneous system of layers as a single medium with anisotropic properties. As discussed previously, this is only valid when the flow extends across many layers. Alternatively, (2.103) is also a valid model for rocks which are genuinely anisotropic, as can happen when sedimentary layers undergo compaction due to high lithostatic pressures (i.e. the weight of overlying rock) over very long time scales. In either case, such a model is relevant to many real flow scenarios in porous media.

2.2.8 Injection into anisotropic media

Consider the injection Q of CO_2 into a two-dimensional anisotropic porous medium with permeability field $\underline{\underline{\mathbf{k}}} = \mathrm{diag}(k_\parallel, k_\perp)$ in the x, z directions. As before, we consider that the flow is bounded above by a horizontal impermeable cap rock located at $z = 0$. Due to the continuity equation, the pressure satisfies

$$k_\parallel p_{xx} + k_\perp p_{zz} = 0, \tag{2.104}$$

within the injected fluid. By switching to a stretched coordinate system

$$\xi = \alpha^{1/4} x, \quad \zeta = \alpha^{-1/4} z, \tag{2.105}$$

the pressure then satisfies the standard Laplace equation,

$$p_{\xi\xi} + p_{\zeta\zeta} = 0. \tag{2.106}$$

The pressure solution (which satisfies suitable flux conditions at the origin) is simply the Green's function in two dimensions

$$p = -\frac{Q\mu}{\pi k_e} \log r + f(t), \tag{2.107}$$

where $r = (\xi^2 + \zeta^2)^{1/2}$, $f(t)$ is some function of time, and $k_e = k_\parallel \alpha^{1/2} = k_\perp \alpha^{-1/2}$ is the effective permeability. This solution does not include the effects of gravity and is therefore only valid very close to the injection point. Hence, this is the appropriate form of the pressure at very early times, when the injected region is very small. This can be seen by comparing the dimensional pressure scaling associated with (2.107) ($Q\mu/k_e$) and the pressure scale associated with the weight of a current of depth H ($\Delta\rho g H$). Hence, (2.107) is valid for currents which satisfy

$$\frac{Q\mu}{k_e} \gg \Delta\rho g H. \tag{2.108}$$

In this case, gravity can be ignored and the appropriate boundary condition for the pressure at the edge of the current is $p = p_a$. By symmetry (since gravity is negligible) the current must grow radially outwards like a circle of radius $R(t)$. Hence, we have

$$p - p_a = -\frac{Q\mu}{\pi k_e} \log \frac{r}{R(t)}. \tag{2.109}$$

The dynamics of the radius are determined by the kinematic condition, which states that

$$\dot{R} = \frac{u_r}{\phi}, \tag{2.110}$$

where u_r is the radial velocity outwards, given by

$$u_r = -\frac{k_e}{\mu} \left.\frac{\partial p}{\partial r}\right|_{r=R(t)} = \frac{Q}{\pi R}. \tag{2.111}$$

Hence, integrating the above two equations gives

$$\frac{1}{2}R^2 = \frac{Qt}{\pi\phi}. \tag{2.112}$$

Note that this equation could also be derived by considering that an injected volume Qt (per unit depth) must occupy a semicircle of area $\phi\pi R^2/2$.

In the original coordinate system the radius satisfies

$$R^2 = \xi^2 + \zeta^2 = x^2\alpha^{1/2} + z^2\alpha^{-1/2}. \tag{2.113}$$

Hence, the shape of the injected flow is actually an ellipse with semi-major and semi-minor axes

$$R_H = R\alpha^{-1/4}, \quad R_V = R\alpha^{1/4}. \tag{2.114}$$

Since $\alpha \leq 1$, the ellipse is always elongated in the horizontal direction (H) and squashed in the vertical direction (V). Hence, the effect of anisotropy is to create a long-thin elliptical flow (but not hydrostatic, as is typically assumed for long-thin flows!).

Next, we consider the effects of gravity. From the earlier analysis (2.108) it is clear that the effects of gravity are appreciable when

$$R_V \approx \frac{Q\mu}{k_e\Delta\rho g} = \frac{Q}{K_e}, \tag{2.115}$$

where $K_e = k_e\Delta\rho g/\mu$ is the effective conductivity. From (2.112),(2.114), this happens at a time

$$t = \frac{\pi\phi Q}{2K_e^2\alpha^{1/2}}. \tag{2.116}$$

Hence, writing everything in terms of the conductivity in the parallel direction $K = k_\parallel\Delta\rho g/\mu$ (which is the most commonly used), we see that the solution regime is determined by two critical parameter values for R_V and t, which are

$$R_V^* = H^* := \frac{Q}{\alpha^{1/2}K}, \quad t^* := \frac{\pi\phi Q}{2\alpha^{3/2}K^2}. \tag{2.117}$$

The regimes are summarised as follows: At early times $t \ll t^*$ (or when $R_V \ll H^*$) the flow is dominated by injection and gravity is negligible; at late times $t \gg t^*$ (or when $R_V \gg H^*$) the flow is dominated by gravity. In the latter case, the earlier gravity current analysis (i.e. (2.66)) is applicable, for which self-similar solutions exist in which $x \sim t^{2/3}$ and $z \sim t^{1/3}$.

This analysis illustrates that the effect of anisotropy is to delay the time at which gravity dominates the flow. Indeed for very heterogeneous/anisotropic geological reservoirs, for which $\alpha = \mathcal{O}(10^{-4})$, the CO_2 current may not feel the effects of gravity until several years after injection begins. This is very important to know, both from the perspective of efficiency as well as safety, before selecting a geological reservoir for carbon storage. Hence, detailed measurements are taken in as many locations as possible, in conjunction with seismic surveys, to assess the landscape of heterogeneities.

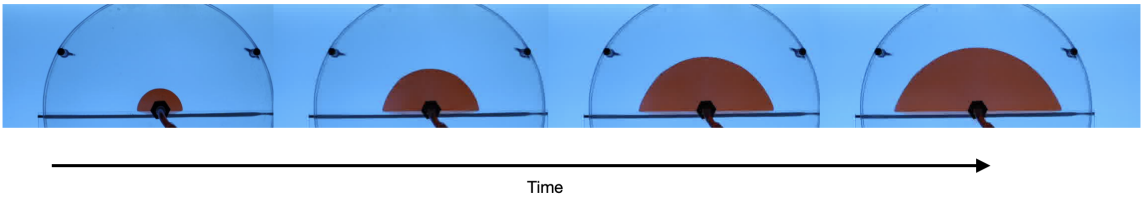

Figure 2.11: Experiments of glycerol (dyed red) injected into a Hele-Shaw cell, aligned vertically so gravity acts downwards. The flow is bounded below by an impermeable substrate.

Despite the simplicity of this problem, we have shown that there exist two separate self-similar regimes. These are summarised by the horizontal and vertical extents of the current R_H and R_V. Hence we have

$$R_H/H^* \propto \begin{cases} (t/t^*)^{1/2}: & t \ll t^*, \\ (t/t^*)^{2/3}: & t \gg t^*, \end{cases}$$
$$R_V/H^* \propto \begin{cases} (t/t^*)^{1/2}: & t \ll t^*, \\ (t/t^*)^{1/3}: & t \gg t^*. \end{cases} \tag{2.118}$$

Snapshots taken from an experiment of glycerol injected between two glass plates (known as a Hele-Shaw cell) are shown in Fig. 2.11. This is the inverted version of a CO_2 current since glycerol is heavy compared with the surrounding air, so gravity causes it to slump downwards. At early times (towards the left of the figure) the current grows like a semi-circle, whereas at late times (towards the right of the figure) the current collapses into a classical gravity current, exactly as we have predicted here.

A similar analysis can be performed in three dimensions, assuming an axisymmetric injection. In this case, different scalings are derived. For example, at early times we have an ellipsoid with

$$R_H = \alpha^{-1/6}R, \quad R_V = \alpha^{1/3}R, \tag{2.119}$$

where $R = (3Qt/4\pi\phi)^{1/3}$ and the transition scalings

$$H^* = \left(\frac{Q}{K}\right)^{1/2}, \quad t^* = \frac{2\pi\phi}{3\alpha}\left(\frac{Q}{K^3}\right)^{1/2}. \tag{2.120}$$

2.3 Unsaturated soils

Let us now consider flow in the unsaturated zone. Above the water table, water and air occupy the pore space. If the porosity is ϕ and the water volume fraction per unit volume of soil is W, then the ratio $S = W/\phi$ is called the *relative saturation*. If $S = 1$, the soil is saturated, and if $S < 1$ it is unsaturated. The pore space of an unsaturated soil is configured as shown in figure 2.12. In particular, the air/water